scientific reports

Check for updates

OPEN

# Concurrent heat stress and air pollution episodes by considering future projection of climate change

Tarkan Alisoltani, Majid Shafiepour Motlagh✉ & Khosro Ashrafi

**The simultaneous effect of heat stress and air pollutants such as ozone can cause many health issues in cities. The situation exacerbates in the context of climate change and temperature rise. Furthermore, ground-level ozone, worsened by climate change, needs investigation for effective management. Therefore, this study projects heat stress and ozone levels in two Coupled Model Intercomparison Project Phase 6 (CMIP6) climate scenarios, SSP245 and SSP585. Results indicate heightened heat stress with increased ozone levels, especially in severe climate scenarios like SSP585. Besides, the study shows that in the SSP245 and SSP585 scenarios, the seasonal shift of high Heat Index (HI) values as well as high ozone concentrations is happening toward the previous months of June-July-August (JJA). High values in the HI classification and the Maximum Daily 8-hour average (MDA8) ozone happen sooner in the March-April-May (MAM) months than the expected JJA months. Furthermore, in the SSP585 scenario, the HI classification above 105 (very hot equal to danger category) is 10% high in all months in comparison to the SSP245 scenario. The study emphasizes the importance of understanding the interactions between heat stress and ozone pollution for implementing effective adaptation and mitigation measures.**

**Keywords** Heat stress, Climate change, Ground level ozone concentration, Air pollution

Recent studies indicate that increased air pollution and extreme heat individually contribute to increased health risks; however, their combined impact is notably more severe[1–3]. The potential interaction between air pollution and heat has been reported, particularly concerning mortality rates. This becomes particularly relevant within the broader context of global climate change[4].

Ozone is mainly known as a warm season air pollutant, whereas its dependence on sunlight makes it very sensitive to meteorological and climatic variability[5]. In addition, climate change and temperature rise boost concerns about ground-level ozone concentration, despite air quality control strategies. As the fluctuation of ozone from one year to another depends largely on how warm and dry the summer is; intense heatwaves can lead to peak ozone values[5]. So, the temperature can be used to predict meteorological factors affecting surface ozone formation[6–11]. Furthermore, temperature rise also has a worsening effect on the comfort zone. With rising temperatures from climate change, heat stress is predicted to intensify, particularly in urban areas due to the urban heat island effect[12].

The variation in global temperature rise scenarios significantly impacts human well-being, with higher temperatures increasing the risk of severe weather events like extreme heat. Detailed and localized information about future climate can be sensible with downscaling methods of climate models. Climate models, which simulate the Earth's climate system, typically operate at coarse spatial resolutions because of computational constraints. Global climate models (GCMs) offer valuable insights into large-scale climate patterns but lack the ability to capture fine-scale variations that are crucial for regional and local decision-making. To provide a framework for comparing and evaluating the outputs of various GCMs, Coupled Model Intercomparison Project Phase (CMIP) is an international effort in climate modeling. Moreover, CMIP6 refers to the sixth phase of this project, which includes the latest generation of climate models, including various GCMs contributed by different research institutions. Besides, it provides significant advantages that combine representative concentration pathways (RCPs) with shared socioeconomic pathways (SSPs), model advancement, and better modeling of synoptic processes.

Future projections of tropospheric O3 under climate change are often carried out using climate chemistry models linked with general circulation models and regional climate models (a recent overview is given[13]). As ozone is a warm season pollutant and is affected by temperature rise, the projected ozone in the presence of other factors is less discussed.

University of Tehran, Tehran, Iran. ✉email: Shafiepour@ut.ac.ir

As discussed in the previous literature, although there are many studies addressing the relationship between ozone concentration and temperature, inquiries persist concerning the evolution of this association over time, across different locations, and in relation to precursor emissions. In addition, the climate change projection of ozone pollutant considering its chemistry and the performance of the downscaling models at different regional scales has not been comprehensively discussed.

To answer the aforementioned question, this study aims to project tropospheric ozone pollutant as a factor of air quality in CMIP6 SSP scenarios and evaluate how it performs compared to heat stress resulted from climate change temperature rise in the megacity of Tehran. Tehran is the Capital of Iran with poor air quality, dust storms as well as temperature rise[14], and reduced average rain fall. Studies show that although mobile and resident sources play an important role in the release of precursors of ozone in Tehran, the results also indicate a significant effect of meteorological conditions on the changes in ozone concentration[15]. Similar studies for Tehran also show the variability of ozone concentration in different months of the year. Therefore, a monthly heat map tracking tropospheric ozone concentrations revealed the minimum level occurring in December and the maximum level in July. Winter exhibited the lowest seasonal concentrations, while summer recorded the highest concentrations[16]. It is worthy to mention that there are many studies investigating the ozone pollutant trend and short-term prediction in Tehran[17,18], and also predicting ozone independent with temperature in a long term climate change modeling period using ANN technique[19]. However, at the regional scale of Tehran, a gap exists for assessing the performance of climate change downscaling and projecting models for ozone pollutants.

This study is conducted in 4 sections. First of all, data extraction sources as well as methods in three categories of station-based data, reanalysis data set, and Earth System Model (ESM) dataset are discussed separately. Furthermore, heat index calculations and downscaling methods as the two main drivers of the study were explained. The later section is the results and discussion of the projected data in the SSP245 and SSP585 scenarios.

## Methods

### Dataset

*Observed data*

In this study, station based hourly reported ozone pollutants in ppb extracted from the Air Quality Control Company (AQCC) of Tehran, from 2013 to 2022 for the JJA period is used. The data was extracted for Sharif University Station, because it has the longest data record. The extracted hourly O3 concentration was in ppb, so it was converted to the 8-hour maximum daily average (MDA8). It's noteworthy to say that ozone is evaluated for 8 h because it reflects cumulative exposure and provides a more accurate assessment of health risks[20].

The heat stress analysis is based on meteorological data of temperature and humidity for synoptic Mehrabad Station, obtained from the Iran Meteorological Organization (IRMO) from 1979-2014.2.1.2. Reanalysis and projection data.

In the downscaling model of the study, the predictor data were meteorological variables retrieved from ERA5 reanalysis data. The meteorological variables were selected to predict ozone concentration based on a similar study[13]. Following this, specific humidity (SH850), temperature (T850), geopotential height (GH850), and vertical as well as horizontal components of the wind (VW850, UW850) were chosen. For this purpose, the aforementioned data was extracted from the European Center for Medium-Range Weather Forecasts dataset. Data was downloaded for the area of study at 850 hPa and for the years between 2013 and 2022 on a daily time scale.

The other predictor for MDA8 ozone pollutant was the ozone concentration in 850 hPa from Copernicus Atmosphere Monitoring Service (CAMS) reanalysis from the European Centre for Medium-Range Weather Forecasts (ECMWF). For ozone projection levels, monthly average ozone data from the BCC-CSM2-MR climate model under the SSP scenario for the time period between 2015 and 2100 and grid type of the study area is downloaded from the USGS database. the BCC-CSM2-MR climate model, models with O3 prescribed from a data set and as part of CMIP6. Hence, there exists a dataset encompassing comprehensive three-dimensional information for both the stratosphere and troposphere. This dataset spans from pre-industrial eras to the current time and extends to the conclusion of the 21st century across different Shared Socioeconomic Pathway (SSP) scenarios[21]. Therefore, for these kinds of models with no interactive chemistry model, an O3 dataset is provided as part of the Chemistry Climate Initiative (CCM). The CCMI aims to conduct a detailed evaluation of participating models using process-oriented diagnostics derived from observations[22]. This data was also implemented on a monthly resolution from 2013 to 2022 and also from 2022 to 2100.

The Climate Model Intercomparison Project Phase 6 (CMIP6) models for meteorological parameters in heat index calculation and the ozone projection downscaling model is used. Therefore, the results of a recent study[23]) are implemented that evaluated the performance of CMIP6 models to select the most suitable model among others in Iran. In this study, 30 models of CMIP6, considering TCR and ECS, were evaluated to investigate temperature spatial distribution and annual trends in Iran with data from Iran's 51 synoptic stations for the historical period (1980–2014). Results showed that four models, including CanESM5, INM-CM5-0, TaiESM1, and UKESM1-0-LL, have shown the highest performance in estimating the temperature in Iran[23]). Thus, the Canadian Earth System Model Version 5 (CanESM5) model was used. Besides, note that due to the implementation of the Heat Index (HI) and ozone definitions and concepts, the modeling period focused on the warm months of the year, particularly the June, July, and August (JJA) months.

## Analysis

According to the flowchart presented in Fig. 1, this research has been conducted using three data sets, which are detailed in the previous sections. This section outlines the steps and methods used in this research.

*HI calculation*

In this study, the NOAA Heat Index (HI) is used to quantify the heat stress concept. Accordingly, the computation of heat index is based on multiple regression analysis that originated from Lans P. Rothfusz[24]. Rothfusz describes the regression equation as follows (Eq. 1):

$$\begin{aligned} \mathrm{HI} = & -42.379 + 20.04901523 * \mathrm{T} + 10.14333127 * \mathrm{RH} - .22475541 * \mathrm{T} * \mathrm{RH} \\ & - 0.00683783 * \mathrm{T} * \mathrm{T} - 0.05481717 * \mathrm{RH} * \mathrm{RH} + 0.00122874 * \mathrm{T} * \mathrm{T} * \mathrm{RH} \\ & + 0.00085282 * \mathrm{T} * \mathrm{RH} * \mathrm{RH} - 0.00000199 * \mathrm{T} * \mathrm{T} * \mathrm{RH} * \mathrm{RH} \end{aligned} \tag{1}$$

Where T is temperature in degrees F and RH is relative humidity in percent. HI is the heat index expressed as an apparent temperature in degrees F. If the RH is less than 13% and the temperature is between 80 and 112 degrees F, it has adjustments in its formula. There are four main classifications for HI values according to NOAA, where HI levels between 80 and 90 are in the Caution group, 91–103 are in the Extreme Caution, 104–124 are in Danger group, 125–137 are in Extreme Danger.

As described in Eq. 1, two meteorological factors of temperature and humidity are coupled in the definition of HI. The selected historical dataset was downscaled using a statistical approach and the CanESM5 model for SSP245 and SSP585 CMIP6 scenarios. As the result, the study evaluated the CMIP6-GCM by comparing it to climatic data and then downscaling it using SDSM for the specific location. Then HI is calculated using Eq. 1.

For the parameter selection, the ERA5 dataset was used to determine the effective parameters in ozone forecasting in the period from 2013 to 2022, as well as the bias correction of the ESM model dataset. Thus, first, a regression model was developed to predict ground level observation ozone with T850, GH850, UW850, VW850, and SH850 parameters, as well as ozone obtained from the CAMS dataset. Based on statistical indicators, it was determined that UW850 and GH850 parameters don't have a special effect on increasing the accuracy and error reduction of the developed regression model. Therefore, they were ignored, and only T850, VW850, and SH850 parameters, along with CAMS ozone, were selected for the next steps. Then these three parameters, extracted from the CanESM5 dataset, were modified based on the ERA5 dataset to develop the final model for projecting surface ozone concentration for the 2023–2100 period. Finally, ozone data from CAMS and three modified parameters (T850, VW850, and SH850) from CanESM5 were used as input and ground-level ozone parameters from Tehran Air Quality Control Company as output to develop a prediction model in the period from 2013 to 2022. The calibrated model by different methods used to predict ground level ozone observations in Tehran by ozone dataset from BCC-CSM2-MR and three modified parameters (T850, VW850, and SH850) from CanESM5 as predictor for the 2023–2100 period.

*Statistical downscaling*

There are many statistical downscaling approaches presented and compared in different studies[26]. In our study, according to[13] to assess future changes of local ground-level O3, the statistical downscaling framework was based on the Perfect Prognosis (PP) approach and is implemented in the urban area of Tehran City. Perfect

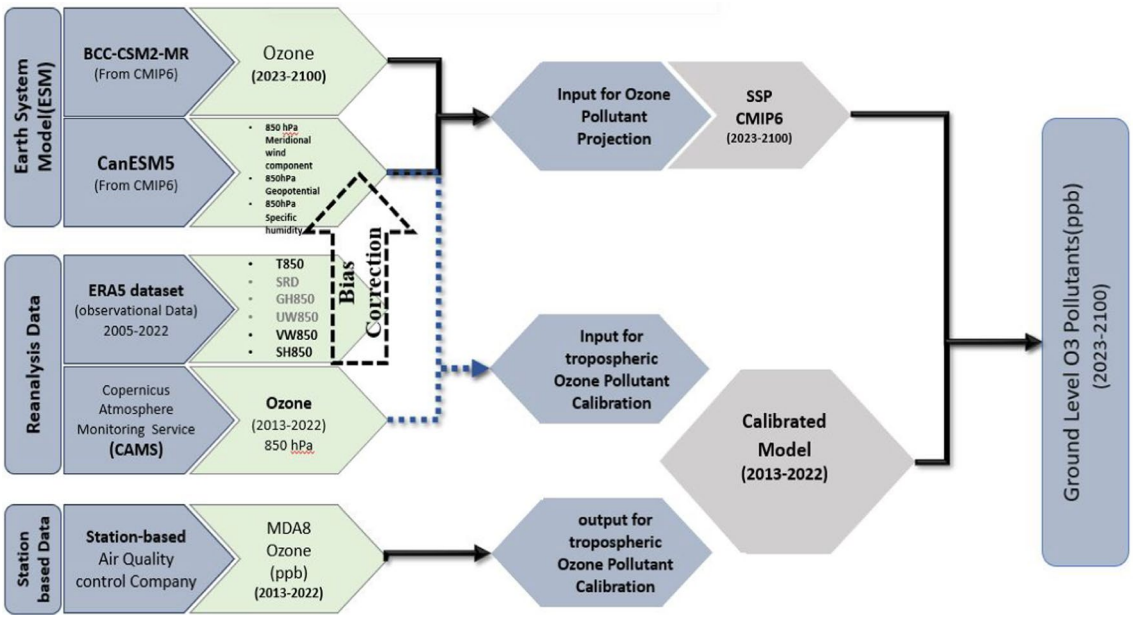


**Fig. 1**. Schematic diagram of the study for ozone projection.

prognosis (PP) statistical downscaling uses synoptic meteorology and climatology to simulate regional climate, analyzing the relationship between synoptic scale and regional weather[27]. In this approach, maximum daily averages 8-hr values (MDA8) is established as the target value.

To generate statistical projections for future climate and emission scenarios, a methodology involved replacing reanalysis predictor data with bias-corrected Earth System Model (ESM) output in Multiple Linear Regression (MLR) models. The focus was on two selected future scenarios, SSP245 and SSP585, during the periods of 2041–2060 and 2081–2100, and with the reference historical period of 2003–2019. This approach aimed to highlight the local changes in ozone (O3) levels anticipated under the influence of projected climate change, providing an understanding of the potential impacts on atmospheric composition in the specified timeframes.

For prediction of station-based scenarios, various machine learning functions were used. The models encompass Artificial Neural Network (ANN), ensemble method (ENS), Regression linear (REG), Support Vector Machin algorithm (SVM), Gaussian Process Regression (GPR), and M5 tree-based machine learning methods (M5tree). For this purpose, the predictor was chosen as ozone obtained from the CAMS (2013–2022) database and meteorological parameters from ERA5, and the predictand was station base MDA8 ozone concentrations. Therefore, the aforementioned machine learning techniques with the specified predictand and predictors resulted in the modeling of SSP scenarios of CMIP6 ozone levels. The machine learning model for ozone pollutant was trained using a 5-fold cross validation method, with 70% data for calibration and 30% for validation.

## Results and discussion

### Heat stress projections

HI levels projecting in different scenarios of the CMIP6 CanESM5 model for SSP245 and SSP585 is shown in Fig. 2. In spite of the approximately similar trends in all modeled scenarios in the initial years of modeling (2020 to 2050), their difference becomes much more evident in the 2050 to 2100 years. The initial shift in SSP245 and the decreasing values in modeling timescale among other SSPs are well aligned with many similar study results[28–30]. Besides, in the SSP585 scenario, the HI classification above 105 (very hot equal to danger category) is 10% high in all months in comparison to SSP245. HI levels above 105 have a general effect on people in high-risk groups. These effects are listed as sunstroke, heat cramps, or heat exhaustion likely, and heatstroke possible with prolonged exposure and/or physical activity[31]. This indicates that in the scenario, which represents high population growth, rapid economic development, and limited climate mitigation efforts (SSP585), health issues from heat stress resulted from global warming become more critical.

Table 1 shows the number of days with different levels of HI in each scenario in two modeling timescales. The SSP245 scenario indicates a "normal" classification of HI (0–80) of 1077 days during the MAM months of 2040–2060. This number reaches 736 with a 31.6% reduction in the later years of modeling (2080–2100). Besides, the MAM months show an increasing trend in the number of days in each classification of hot to extreme hot (80–130) levels of HI. The trend shows a total + 28.5% increment in the number of the days in 80–130 HI for the periods 2041–2060 and 2081–2100. On the contrary, the SON months have a decreasing number of days in each HI classification in the horizon years of the modeling timescale. The trend shows a total − 19.8% reduction in the number of days in 80–130 HI for the periods 2041–2060 and 2081–2100. In the SSP245 scenario, high HI values shift towards previous JJA months, indicating that high HI classification values occur earlier than expected JJA months. This is also evident in Fig. 3. According to Fig. 3a, the number of days with lower HI values gradually decreases, while the number of days with higher HI values increases. Analyzing this figure reveals that the days with HI in the caution classification gradually increase, and their peak shifts towards the earlier months of the year. In other words, a seasonal shift, referring to the movement of months with discomfort HI index to the earlier in the year, is occurring. SSP585 scenario also shows that the number of days in HI classification from extreme caution to extreme danger (90 to 130) in MAM months of 2080–2100 is + 50% more than 2040–2060 (Table 1). This ratio is so small (less than 1%) in other months. It can be understood that in SSP585, as time passes, exposing extreme caution to extreme danger happens sooner than JJA months. In this scenario, as illustrated in Fig. 3b, an increase in the number of days with HI in caution classification in JJA

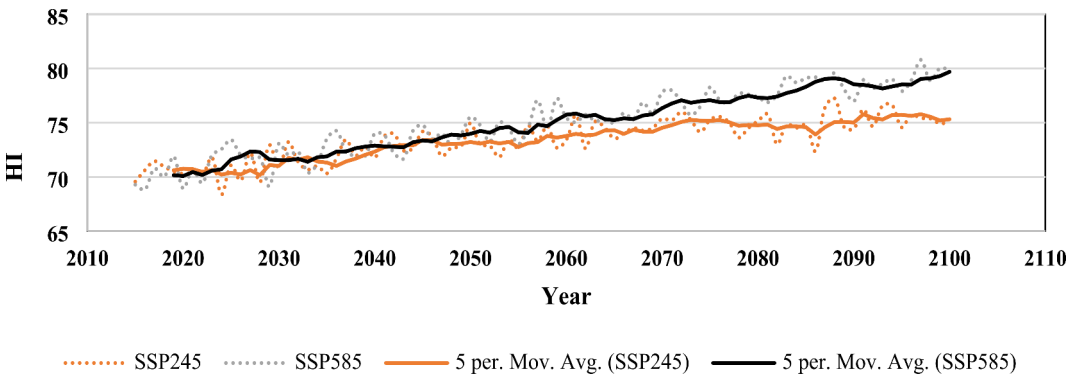


**Fig. 2**. HI levels projecting in different scenarios of the CMIP6 CanESM5 model for SSP245 and SSP585 for the city of Tehran, Iran.

| Projected Modeling timeframe | Months | 0–80 | | 80–90 | | 90–105 | | 105–130 | | > 130 | |
|---|---|---|---|---|---|---|---|---|---|---|---|
| | | SSP245 | SSP585 | SSP245 | SSP585 | SSP245 | SSP585 | SSP245 | SSP585 | SSP245 | SSP585 |
| 2040–2060 | March, April, May | 1077 | 1079 | 411 | 438 | 389 | 375 | 55 | 40 | 0 | 0 |
| 2080–2100 | | 736 | 561 | 463 | 533 | 507 | 518 | 226 | 320 | 0 | 0 |
| 2040–2060 | Jun, July, Aug | 0 | 0 | 1 | 6 | 446 | 373 | 1484 | 1552 | 0 | 0 |
| 2080–2100 | | 0 | 0 | 0 | 0 | 331 | 96 | 1600 | 1832 | 0 | 3 |
| 2040–2060 | Sep, Oct, Nov | 1204 | 1152 | 343 | 357 | 356 | 385 | 10 | 19 | 0 | 0 |
| 2080–2100 | | 1345 | 1129 | 295 | 351 | 269 | 403 | 4 | 30 | 0 | 0 |

**Table 1**. Number of days based on projected HI classification in SSP245 & SSP585 scenarios (2040–2060 & 2080–2100).

months, and their spread to the spring and autumn, months is observed, along with a seasonal shift causing the HI with caution values in months to occur earlier in the year.

## Ozone projection

Table 2 shows the results of different machine learning models used in this study for predicting ozone levels. Through the comparison of model performances in predicting ozone levels, it was identified that the M5tree and ENSEMBLE models exhibit the best performance based on the *R2* and *RMSE* indices. However, the M5tree model demonstrates lower error and higher accuracy. The reason for this lies in the significantly better performance of this model in higher ozone concentrations. Considering the standards and sensitivity to high ozone levels, a more accurate estimation of higher ozone values is crucial. Therefore, the M5tree model was selected as the best for predicting ozone concentrations in various scenarios. Results show ground-level ozone could be predicted by the ERA5 and CAMS datasets with high accuracy[13,32].

The CMIP6 modeling reveals variability in ground-level ozone concentration in SSP245 and SSP585 scenarios (Fig. 4a,b), indicating the projected concentration of MDA8 ozone during the modeling timescale. The months of June, July, and August, located in the middle of the heat map of ozone have the highest number of exceedance limits among other months. The SSP585 scenario experiences a higher number of ozone pollutant standard deviations than SSP245, particularly in September and before the JJA. The ozone standard level for health for an eight-hour exposure limit is 54 ppb according to the EPA, and more than this limit indicates health issues. Besides, the number of days exceeding the ozone standard level in each scenario in the modeling timeframes (2040–2060 & 2080–2100) is shown in Table 2. In the SSP245 scenario, the number of days of projected MDA8 ozone concentration between 54 and 105 ppb, before the months of JJA (March, April, May), and in the years from 2080 to 2100 is + 20% more than SON (September, October, November) months. Subsequently, the comparison between SON, JJA, and MAM months in two modeling timeframe (2040–2060 and 2080–2100) shows high values of MDA8 ozone concentration in the second period, which happen sooner than JJA months (Table 3). The same trend happens in the SSP585 scenario, representing the outcomes of high-level ozone concentration happening sooner than the original period of JJA months. Studies confirm that temperature rise leads to ozone increases of up to 2.2 ppb over land[33] and that increasing in O3 levels during hot months is also observed in polluted environments[13,32,34–36].

## Concurrent of projected ozone concentration and heat stress

In order to evaluate the simultaneous effect of temperature rise and ozone pollutant levels as the result of climate change in CMIP6 scenarios, the interaction of them for different levels in the modeling years and for SSP245 and SSP585 were assessed (Fig. 5). As shown in the contour plot in both SSP245 and - SSP585 scenarios, the high levels of MDA8 ozone concentration are happening at higher heat stress levels. Besides, the rate of increase in values for both parameters is indicative of the progression over the years.

Analyzing the contour plot of HI and ozone levels in the SSP245 scenario (Fig. 5a), indicates that in lower levels of MDA8 ozone concentrations (0–20 ppb), the values of HI remain constant and in the *caution* level classification by the passing years (less than 80). Furthermore, in the area between 20 ppb and approximately 54 ppb in ozone concentration (still below the standard levels), the HI values vary between 90 and 100 values, representing the *extreme caution* classification. In the initial higher values of ozone concentration above the standard level (54–80 ppb), the HI levels representing *extreme caution* (95–100) increase and reach the *danger* level classification in the period of 2090–2100 years. The number of days representing the *danger* HI classification (more than 105) increases with higher values of ozone concentration and in 2070–2100. For the most part, in the SSP245 scenario, with the indication of assuming implementing climate change mitigation measures, the results are a demonstration of a coupled unhealthy level of ozone pollutant and heat stress starting in the year 2050.

This trend is a little different in the contour plot of HI and ozone levels in the SSP585 scenario (Fig. 5b). The incremental trend of HI values is happening sooner in initial levels of ozone concentration. Besides, the *extreme caution* (91–103) values of HI happen in a greater number of days of modeling timescale (orange clouds), and in the ozone levels above standard (54 ppb). HI levels (above 105) reach sooner to the *danger* classification from

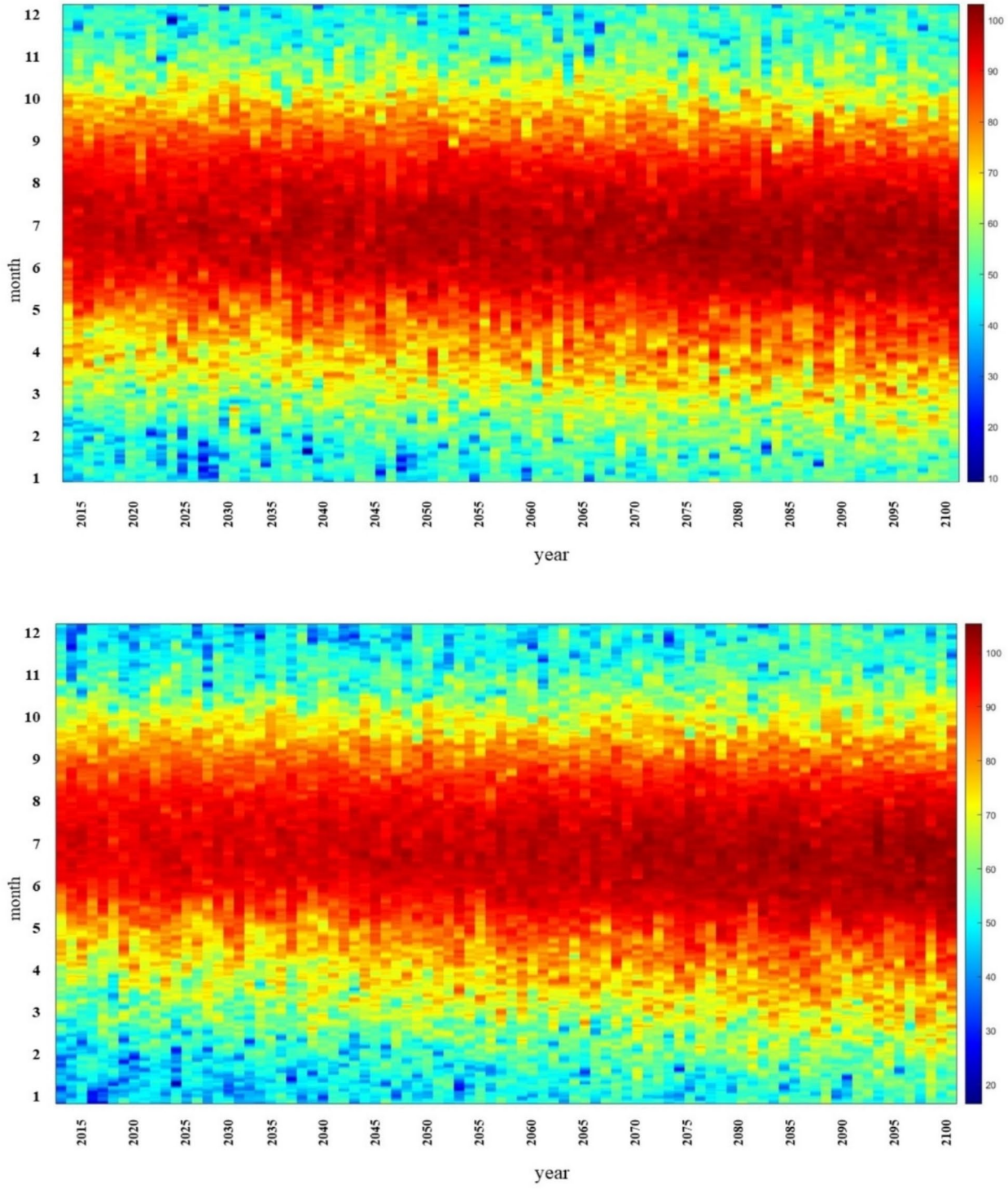


**Fig. 3**. Heat map of projected CMIP6 heat index (°F) in (**a**) SSP245 and (**b**) SSP585 scenarios.

| | ANN | ENS | REG | SVM | GPR | M5tree |
|---|---|---|---|---|---|---|
| $R^2$ | 0.67 | 0.85 | 0.61 | 0.67 | 0.73 | 0.90 |
| RMSE | 9.25 | 6.18 | 10.13 | 9.41 | 8.40 | 5.08 |

**Table 2**. Statistical downscaling model performance for predicting ozone levels.

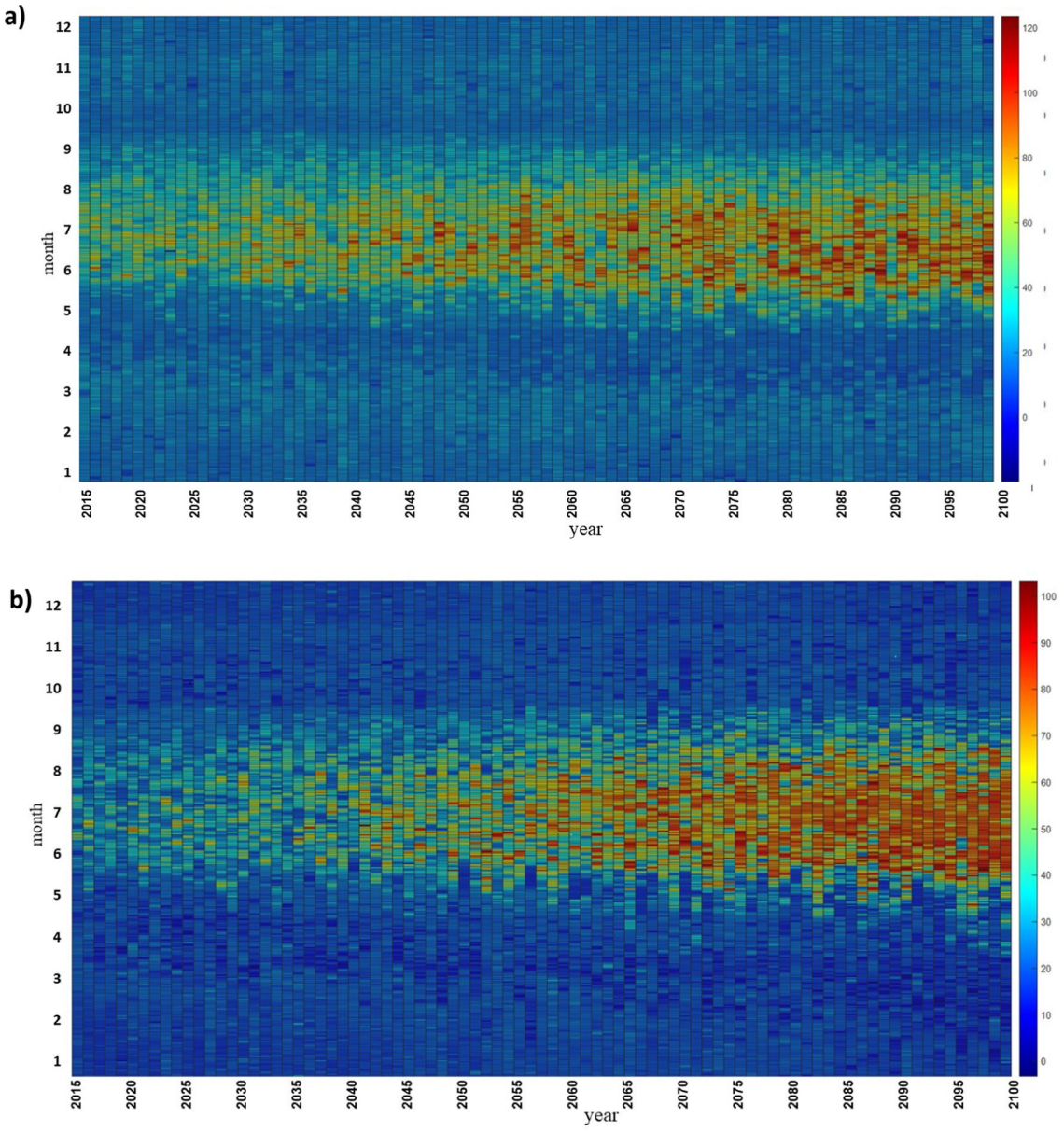


**Fig. 4**. Variability of projected ground-level ozone concentrations (ppb) in scenarios (**a**) SSP245 and (**b**) SSP585 based on CMIP6 modeling.

| Projected Modeling timeframe | Months | 0-54 ppb | | 54-70 ppb | | 70-85 ppb | | 85-105 ppb | | >105 ppb | |
|---|---|---|---|---|---|---|---|---|---|---|---|
| | | SSP245 | SSP585 | SSP245 | SSP585 | SSP245 | SSP585 | SSP245 | SSP585 | SSP245 | SSP585 |
| 2040-2060 | March, April, May | 1921 | 1907 | 9 | 21 | 1 | 4 | 1 | 0 | 0 | 0 |
| 2080-2100 | | 1538 | 1471 | 150 | 138 | 131 | 268 | 100 | 55 | 13 | 0 |
| 2040-2060 | Jun, July, Aug | 991 | 1302 | 490 | 348 | 303 | 215 | 141 | 30 | 6 | 0 |
| 2080-2100 | | 1612 | 1520 | 117 | 133 | 96 | 232 | 97 | 46 | 9 | 0 |
| 2040-2060 | Sep, Oct, Nov | 1912 | 1909 | 0 | 3 | 0 | 0 | 0 | 0 | 0 | 0 |
| 2080-2100 | | 1598 | 1496 | 109 | 92 | 113 | 261 | 86 | 63 | 6 | 0 |

**Table 3**. Number of days exceeding ozone standard level in each scenario 2040–2060 & 2080–2100.

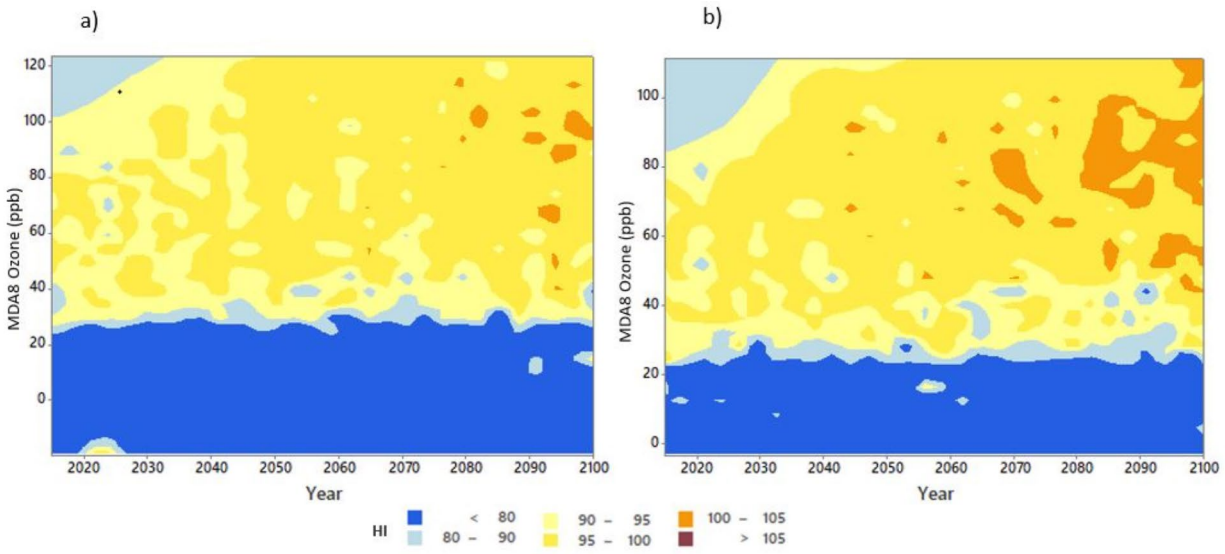


**Fig. 5**. Contour plot of HI and ozone levels from CMIP6 modeling presented in (**a**) SSP245 and (**b**) SSP585 scenarios.

| Projected Modeling timeframe | Months | O3 > 70 | | O3 > 70 and HI > 90 | |
|---|---|---|---|---|---|
| | | SSP245 | SSP585 | SSP245 | SSP585 |
| 2040–2060 | March, April, May | 1 | 4 | 0 | 2 |
| 2080–2100 | | 14 | 323 | 14 | 323 |
| 2040–2060 | Jun, July, Aug | 146 | 245 | 141 | 244 |
| 2080–2100 | | 29 | 278 | 29 | 278 |
| 2040–2060 | Sep, Oct, Nov | 0 | 0 | 0 | 0 |
| 2080–2100 | | 23 | 324 | 23 | 324 |

**Table 4**. Number of days exceeding ozone and heat index levels from comfort interval in each scenario (2040–2060 & 2080–2100).

2040 to 2050 years, indicating a greater possibility of sunstroke, heat cramps, heat exhaustion, and heatstroke in the case of prolonged exposure and/or physical activity in the near-term modeling time.

The simultaneous effect of high ozone concentration (MDA8 Ozone > 54 ppb) and high heat stress values (HI > 90) mainly happens from 2050 to 2100 in both SSP245 and SSP585 scenarios. More occurrence of high values of heat stress coupled with ozone air pollutants is resulting in critical health issues. High ozone levels can cause induction of respiratory symptoms, decrements in lung function, and inflammation of the airways[37], while high values of HI can increase the possibility of heatstroke in the case of long exposure[31] in the outdoors. Results show the increase in the number of days as well as in the period of seasons with exposure to the exceedance level of both HI and Ozone in comparison to the historical period. This can expose serious health problems in the case of the projected climate change scenarios.

Table 4 presents the number of days during which ozone and HI (Heat Index) levels are in the caution and warning statuses. This table includes two scenarios, SSP245 and SSP585, for two time periods, 2040–2060 and 2080–2100. It calculates the number of days when ozone levels exceed 70, and when both ozone levels exceed 70 and HI levels exceed 90. Comparing the results of these two conditions in summer, spring, and autumn reveals that in over 99% of cases, ozone levels above 70 are observed when HI levels are above 90. In other words, ozone levels in the warning state occur only when HI levels are also in the warning state. This finding is also graphically illustrated in Fig. 5. Recent studies also confirm the future increase in heat stress and ozone pollutant due to climate change, which will lead to increased mortality and threaten the health of humans and living organisms[38,39]. However, the interaction of these two important phenomena has been investigated for the first time in this research.

## Conclusion

Climate change, which leads to an increase in temperature and also heat stress, threatens human health. Ground level ozone, which is one of the most important pollutants in hot seasons, is also affected by climate change. Therefore, it is necessary to predict the heat stress and ground level ozone concentrations as the result of

temperature rise that happens in the city scale and climate change context. For this purpose, in this research, heat stress caused by temperature increase was first modeled for SSP245 and SSP585 scenarios. Then, according to the ozone dataset from the CAMS model and ERA5 climate parameters, a model was developed to predict observational ozone (MD8) concentration. Finally, by using the ozone data predicted by the BCC-CSM2-MR CMIP6 model, ground level ozone concentration has been predicted for Tehran. The following results were obtained:

- High values of heat stress occur in high values of ozone concentrations.
- The hot seasonal shift in years is evident in high MDA8 ozone values. The trend shows a seasonal shift toward the previous months of JJA, and the increasing number of days that ozone exceeds the normal level (54 ppb) happens sooner in MAM months.
- It can be understood that in the SSP245 and SSP585 scenarios, the seasonal shift of high HI values is happening toward the previous months of JJA, and high values in the HI classification happen sooner (MAM months) than the expected JJA months.
- The result of projected heat stress in SSP245 and SSP585 scenarios, in the period of 2040–2060 and 2080–2100, shows that the number of days with caution to extreme danger for health ($90 =< HI < 130$) classification increases as the result of climate change. This means that heatstroke possibility because of prolonged exposure increases, and this will not be limited to typical warm months of the year (JJA), but also the HI exceedance levels happen sooner and more often in MAM months.
- The result of projected MDA8 ozone concentration in SSP245 and SSP585 scenarios, in the period of 2040–2060 and 2080–2100, shows more unhealthy days ($> 54$ ppb) happening. This means the health issues related to high ozone levels, like decrements in lung function and induction of respiratory symptoms, happen much more frequently and are not limited to JJA months, but high-level exposure happens sooner in MAM months.
- Specific humidity, V component of wind, and temperature are the most important parameters involved in projecting MDA8 ozone concentrations, and UW850 and GH850 parameters don't have a meaningful effect on projecting MD8 ozone.
- The M5tree model has the best performance and the lowest error in ozone prediction.
- This study indicates that even in the SSP245 scenario considering implementing mitigation pathways, the heat stress levels enter the extreme caution and even exceed 103 in the year 2076. This is also the same as ground level MDA8 ozone concentrations that exceed 123 ppb in the year 2089. The combination of projected MDA8 ozone levels as well as HI levels for different SSP scenarios is analyzed in order to highlight the critical periods of time when they pass threshold levels. Thus, these two parameters are being compared with their national standard level for human health and beings, demonstrating the simultaneity level of these two parameters at high values can be a representation of climate change resiliency. Furthermore, the results highlight that more climate change mitigation measures are expected for the city of Tehran considering its microclimate circumstances, and also, accelerating its developing socio environmental pathways.

Among climate change mitigation pathways, the role of urban planning and urban design to improve microclimates in cities is undeniable. In the city of Tehran, the capital of Iran, as one of the developing countries, climate change mitigation and adaptation measures are implementing in a slow and unplanned trend. Besides, the geometry of Tehran and complex urban morphology of it, make it more vulnerable for heat-island effects[40], which is worsened by its inappropriate city design and street canyon effects.

Urban green spaces (UGS) are crucial for climate change mitigation, enhancing urban quality of life, and promoting environmental justice[41], accessible to all citizens regardless of social and economic status. Socio-economic inequalities, leading to poor spatial configuration, and distribution of UGS[42] worsen the environmental justice measures. Besides, according to the Iran Ministry of Roads & Urban Development's studies, considering the regional climate, the approved per capita urban green space in Iran's urban areas is 7 to 12 square meters per person[43] which is 2.9 square meters lower than world standards[44]. This is a demonstration of low mitigation and adaptation factors against climate change heat stress. Therefore, the results of this research can be used with great confidence to plan and manage the adaptation and mitigation of humans to new conditions caused by climate change.

## Data availability

The datasets used and/or analysed during the current study available from the corresponding author on reasonable request.

Received: 21 May 2024; Accepted: 4 November 2024
Published online: 26 November 2024

## References

1. Lee, W. et al. Synergic effect between high temperature and air pollution on mortality in Northeast Asia. *Environ Res* **178**, 108735 (2019).
2. Zhou, L. et al. The interactive effects of extreme temperatures and PM(2.5) pollution on mortalities in Jiangsu Province, Chin. *Sci Rep* **13**(1), 9479 (2023).
3. De Vita, A. et al. The impact of climate change and extreme weather conditions on cardiovascular health and acute cardiovascular diseases. *Journal of Clinical Medicine* **13**(3), 759 (2024).
4. Qin, R. X. et al. The interactive effects between high temperature and air pollution on mortality: A time-series analysis in Hefei, China. *Science of The Total Environment* **575**, 1530–1537 (2017).
5. Climate-ADAP, T.E.C.A.P. *Ground-level ozone effects on human health under the changing climate*. Available from: https://climate-adapt.eea.europa.eu/en/observatory/evidence/health-effects/ground-level-ozone/ground-level-ozone.

6. Jacob, D. J. et al. Factors regulating ozone over the United States and its export to the global atmosphere. *Journal of Geophysical Research: Atmospheres* **98**(D8), 14817–14826 (1993).
7. Ryan, W. F. et al. Pollutant transport during a regional O3 episode in the mid-Atlantic states. *Journal of the Air & Waste Management Association* **48**(9), 786–797 (1998).
8. Meng, X. et al. Chemical drivers of ozone change in extreme temperatures in eastern China. *Science of The Total Environment* **874**, 162424 (2023).
9. Nussbaumer, C. M. & Cohen, R. C. The role of temperature and NO x in ozone trends in the Los Angeles Basin. *Environmental Science & Technology* **54**(24), 15652–15659 (2020).
10. Shi, W. et al. Modification effects of temperature on the ozone–mortality relationship: a nationwide multicounty study in China. *Environmental Science & Technology* **54**(5), 2859–2868 (2020).
11. Sillman, S. The relation between ozone, NOx and hydrocarbons in urban and polluted rural environments. *Atmospheric Environment* **33**(12), 1821–1845 (1999).
12. Oleson, K. W. et al. Interactions between urbanization, heat stress, and climate change. *Climatic Change* **129**(3), 525–541 (2015).
13. Hertig, E., Jahn, S. & KasparOtt, I. Future local ground-level ozone in the european area from statistical downscaling projections considering climate and emission changes. *Earth's Future* **11**(2), e2022EF003317 (2023).
14. Roshan, G. & Nastos, P. T. Assessment of extreme heat stress probabilities in Iran's urban settlements, using first order Markov chain model. *Sustainable Cities and Society* **36**, 302–310 (2018).
15. Borhani, F. et al. Tropospheric Ozone in Tehran, Iran, during the last 20 years. *Environmental Geochemistry and Health* **44**(10), 3615–3637 (2022).
16. Borhani, F. et al. Current status and future forecast of short-lived climate-forced ozone in Tehran, Iran, derived from ground-based and satellite observations. *Water, Air, & Soil Pollution* **234**(2), 134 (2023).
17. Motesaddi Zarandi, S. et al. Long-term trends of Nitrogen oxides and surface ozone concentrations in Tehran city, 2002–2011. *Journal of Environmental Health Science and Engineering* **13**(1), 63 (2015).
18. Masoudi, M., Behzadi, F. & Sakhaei, M. Status and prediction of Ozone as an air pollutant in Tehran. *Iran. Ecology Environment and Conservation* **20**(2), 775–780 (2014).
19. Mosadegh, E., et al., *Modeling the Regional Effects of Climate Change on Future Urban Ozone Air Quality in Tehran, Iran*. 2021.
20. (EPA), E.P.A., *Eight-Hour Average Ozone Concentrations*. January 19, 2024.
21. Keeble, J., et al., *Evaluating stratospheric ozone and water vapor changes in CMIP6 models from 1850–2100*. 2020.
22. Morgenstern, O., et al., *Review of the global models used within the Chemistry-Climate Model Initiative (CCMI)*. Geoscientific Model Development Discussions, 2016: p. 1–49.
23. Zarrin, A. & Dadashi-Roudbari, A. Evaluation of CMIP6 models in estimating temperature in Iran with emphasis on equilibrium climate sensitivity (ECS) and transient climate response (TCR). *Iranian Journal of Geophysics* **17**(1), 39–56 (2023).
24. Rothfusz, L.P., *The Heat Index "Equation"n(or, More Than You Ever Wanted to Know About Heat Index)*, S.S. Division, Editor. 1990, NWS Southern Region Headquarters, Fort Worth, TX.
25. Organization, I.M., a.o.t.M.o.R.a.U.D.o.t.G.o.I. Met Department, Editor.
26. Gutiérrez, J. M. et al. An intercomparison of a large ensemble of statistical downscaling methods over Europe: Results from the VALUE perfect predictor cross-validation experiment. *International Journal of Climatology* **39**(9), 3750–3785 (2019).
27. *Perfect Prognosis*, in *Statistical Downscaling and Bias Correction for Climate Research*, D. Maraun and M. Widmann, Editors. 2018, Cambridge University Press: Cambridge. p. 141–169.
28. Li, H., et al., Drylands face potential threat of robust drought in the CMIP6 SSPs scenarios. *Environmental Research Letters*, 2021. **16**.
29. Christian, J. I. et al. Global projections of flash drought show increased risk in a warming climate. *Communications Earth & Environment* **4**(1), 165 (2023).
30. Yousefpour, R. and Hanewinkel, M. Climate change and decision-making under uncertainty. *Current Forestry Reports*, 2016. **2**.
31. (NOAA), N.O.a.A.A., *Heat Index ChartHeat Index Chart*.
32. Jahn, S. & Hertig, E. Modeling and projecting health-relevant combined ozone and temperature events in present and future Central European climate. *Air Quality, Atmosphere & Health* **14**, 563–580 (2021).
33. Kim, M. J. et al. Future ozone and oxidants change under the RCP scenarios. *Atmospheric Environment* **101**, 103–115 (2015).
34. Hertig, E. Health-relevant ground-level ozone and temperature events under future climate change using the example of Bavaria, Southern Germany. *Air Quality, Atmosphere & Health* **13**(4), 435–446 (2020).
35. Schnell, J. L. et al. Effect of climate change on surface ozone over North America, Europe, and East Asia. *Geophysical research letters* **43**(7), 3509–3518 (2016).
36. Lin, M. et al. US surface ozone trends and extremes from 1980 to 2014: Quantifying the roles of rising Asian emissions, domestic controls, wildfires, and climate. *Atmospheric Chemistry and Physics* **17**(4), 2943–2970 (2017).
37. Agency(EPA), T.E.P., *Health Effects of Ozone in the General Population*.
38. Chen, L. et al. Increases in ozone-related mortality in China over 2013–2030 attributed to historical ozone deterioration and future population aging. *Science of The Total Environment* **858**, 159972 (2023).
39. Orru, H. et al. Ozone and heat-related mortality in Europe in 2050 significantly affected by changes in climate, population and greenhouse gas emission. *Environmental Research Letters* **14**(7), 074013 (2019).
40. Alizadeh-Choobari, O., Ghafarian, P. & Adibi, P. Inter-annual variations and trends of the urban warming in Tehran. *Atmospheric Research* **170**, 176–185 (2016).
41. Kirschner, V. et al. Measuring the relationships between various urban green spaces and local climate zones. *Scientific Reports* **13**(1), 9799 (2023).
42. Nasri Roodsari, E. & Hoseini, P. An assessment of the correlation between urban green space supply and socio-economic disparities of Tehran districts—Iran. *Environment, Development and Sustainability* **24**, 1–16 (2021).
43. Asgari, A. *Urban Land Use Planning* (Nor Ghalam press, 2001).
44. Arghavani, S., Malakooti, H. & Bidokhti, A. A. Numerical evaluation of urban green space scenarios effects on gaseous air pollutants in Tehran Metropolis based on WRF-Chem model. *Atmospheric Environment* **214**, 116832 (2019).


## Author contributions

T.A., M.S.M. and K.A. wrote the main manuscript text. T.A. prepared all figures and tables. M.S.M. and K.A. reviewed the manuscript.

## Declarations

## Competing interests

The authors declare no competing interests.

## Additional information

**Correspondence** and requests for materials should be addressed to M.S.M.